Springer Proceedings in Materials

U. Kamachi Mudali
S. T. Aruna
H. P. Nagaswarupa
Dinesh Rangappa *Editors*

Recent Trends in Electrochemical Science and Technology

Proceedings of Papers Presented at NSEST-2020 and ECSIRM-2020

Springer

Springer Proceedings in Materials

Volume 15

Springer Proceedings in Materials publishes the latest research in Materials Science and Engineering presented at high standard academic conferences and scientific meetings. It provides a platform for researchers, professionals and students to present their scientific findings and stay up-to-date with the development in Materials Science and Engineering. The scope is multidisciplinary and ranges from fundamental to applied research, including, but not limited to:

- Structural Materials
- Metallic Materials
- Magnetic, Optical and Electronic Materials
- Ceramics, Glass, Composites, Natural Materials
- Biomaterials
- Nanotechnology
- Characterization and Evaluation of Materials
- Energy Materials
- Materials Processing

To submit a proposal or request further information, please contact one of our Springer Publishing Editors according to your affiliation:

European countries: **Mayra Castro** (mayra.castro@springer.com)
India, South Asia and Middle East: **Priya Vyas** (priya.vyas@springer.com)
South Korea: **Smith Chae** (smith.chae@springer.com)
Southeast Asia, Australia and New Zealand: **Ramesh Nath Premnath** (ramesh.premnath@springernature.com)
The Americas: **Michael Luby** (michael.luby@springer.com)
China and all the other countries or regions: **Mengchu Huang** (mengchu.huang@springer.com)

More information about this series at https://link.springer.com/bookseries/16157

U. Kamachi Mudali · S. T. Aruna ·
H. P. Nagaswarupa · Dinesh Rangappa
Editors

Recent Trends in Electrochemical Science and Technology

Proceedings of Papers Presented at NSEST-2020 and ECSIRM-2020

Springer

Editors
U. Kamachi Mudali
VIT Bhopal University
Bhopal, Madhya Pradesh, India

H. P. Nagaswarupa
Department of Chemistry
Davangere University
Tholahunase, Karnataka, India

S. T. Aruna
Surface Engineering Division
National Aerospace Laboratories
Council of Scientific and Industrial
Research
Bengaluru, Karnataka, India

Dinesh Rangappa
Department of Applied Sciences
Visvesvaraya Technological University
Chickballapur, Karnataka, India

ISSN 2662-3161 ISSN 2662-317X (electronic)
Springer Proceedings in Materials
ISBN 978-981-16-7553-9 ISBN 978-981-16-7554-6 (eBook)
https://doi.org/10.1007/978-981-16-7554-6

This Springer imprint is published by the registered company Springer Nature Singapore Pte Ltd.
The registered company address is: 152 Beach Road, #21-01/04 Gateway East, Singapore 189721, Singapore

Contents

About the Editors

Dr. U. Kamachi Mudali Vice-Chancellor of VIT Bhopal University & Honorary Professor of Practice, IIT Madras is formerly Distinguished Scientist of Department of Atomic Energy (DAE), and Chief Executive & Chairman of Heavy Water Board, a flagship industrial unit of DAE. Dr. Mudali made pioneering contributions to advanced materials & coating technology development; corrosion science, engineering and technology; materials, process and equipment development for reprocessing applications; failure analysis, consultancy and societal contributions. He has 465 journal publications, five patents, and 9740 citations with an h-index of 44 and i-10 index of 246. He is recognized in the World's Top 2% scientists from India in the field of Materials, and is a Fellow of 12 professional associations. He has guided/coordinated 162 UG, PG and PhD students, and has published 21 Books/Proceedings. Dr. Mudali is decorated with several distinguished recognitions from India and abroad including: Distinguished Alumnus Award from IIT Bombay where he did M.Tech. (Corrosion Science and Engineering) in 1984, and PSG College of Technology, Coimbatore where he did M.Sc. (Materials Science) in 1982, GD Birla Gold Medal and Metallurgists of the Year Award from IIM & GoI, MASCOT National Award, Vasvik Award, INS Medal, Outstanding Faculty Award of HBNI, Homi Bhabha Science and Technology Award of Department of Atomic Energy, Fellow & Frank Newman Speller Award of NACE International, USA, the highest recognition and first Indian to get in the field of corrosion.

Dr. S. T. Aruna is currently working as a Senior Principal Scientist at Council of Scientific and Industrial Research—National Aerospace Laboratories (CSIR-NAL), Bangalore, India. She has a Master's Degree in Chemistry from Mysore University (1994) and she secured the first rank and won four gold medals. She obtained her Ph.D. from the Indian Institute of Science (IISc), Bangalore in 1998. She worked as a postdoctoral fellow at Bar-Ilan University, Israel in the area of dye-sensitized solar cells from 1998–1999. She has authored ~106 research papers in international peer-reviewed journals, nine patents, co-authored a book and written ten book chapters and four encyclopedia chapters. Her research papers have been well-cited and her publications have an h-index of 40. Her name featured among 1494 Indian scientists

in the list of top 2% of the world scientists released by Stanford University in January 2021. Her current research interests include the development of tapecast ceramic substrates for electronics application, nanomaterials, plasma sprayed thermal and environmental barrier coatings, oxygen sensor and solid oxide fuel cells (SOFCs). She has guided five Ph.D. and 25 Masters' Students.

Dr. H. P. Nagaswarupa is currently an Associate Professor in the Department of Studies in Chemistry, Davangere University, India. He obtained his Master's degree in Chemistry from Bangalore University (2002) and Ph.D. degree from Bharathidasan University, Trichy (2012). He has been teaching Chemistry for the undergraduate and postgraduate level since 18 years. He has guided three Ph.D. students and currently guiding six Ph.D. students. He has published over 160 research papers in national/international journals and holds three patents. His papers are well cited with an h-index of 31. He has organized more than 25 workshops/conferences at the national/international level. He is also a member of various committees for the inspection of new as well as old institutions. His areas of interest include Nano Science & Technology, Materials Science and Corrosion Science.

Prof. Dinesh Rangappa received his M.Sc. and Ph.D. in Environmental Science from the University of Mysore, India. He obtained his second doctoral degree Dr. Engg., (Materials Science and Engineering, 2004) from Tokyo Institute of Technology, Japan. He has received JSPS Research Fellow award at AIST, Japan. He was deputed to Visvesvaraya Technological University (VTU), as a Special officer and PG Coordinator for VTU Bangalore Region. Since 2013, he is serving as Professor and Chairman, Department of Nanotechnology, VTU. Professor Rangappa has significantly contributed to developing a novel process for bulk production of nanomaterials, engineering nanomaterials for energy storage, sensors and photovoltaic, photocatalysis, photoluminiscent, inorganic Nano-pigment, wastewater treatment and biomedical applications. He has published more than 120 papers in national and international journals (h-index-23), eight book chapters and two patents granted. He has been awarded Prof. Satish Dhawan Karnataka State Award for Young Engineers—2014, Pavan Nagapal Memorial Award 2015 and Gandhian Young Technological Innovation Award 2016, and Japan Society for the Promotion of Science (JSPS) Bridge Fellowship Award 2017.

Benzotriazole Encapsulated Nanocontainer-Based Self-healing Coatings for Corrosion Protection of Mild Steel

Aarti Gautam, K. R. C. Soma Raju, K. V. Gobi, and R. Subasri

1 Introduction

Mild steel is one of the extensively used materials in industrial sectors because of its ease of availability and low cost. Mild steel is regarded as one of the desired materials for construction because of its excellent mechanical properties such as ductility, tensile strength, etc. [1]. The presence of low carbon content makes it more efficient to be used in areas where high-temperature conditions are required. Mild steel is highly malleable and hence finds its use in oil and pipeline industries. However, it is prone to get oxidized and to undergo corrosion as soon as it comes in contact with air, moisture, acids, etc., and all these could lead to changes in physical appearance, reduced mechanical strength, and structural deformation, which could cause severe accidents [2].

Hence, protection is necessary to prevent the surface from being corroded. Hexavalent chromate conversion coatings (CCC) and phosphate coatings are effective for protecting the metal surfaces, as they impart excellent corrosion resistance properties and are cost-effective [2, 3]. Even though they are considered the best protection

A. Gautam (✉) · K. R. C. Soma Raju · R. Subasri
Centre for Sol-Gel Coatings, International Advanced Research Centre for Powder Metallurgy and New Materials (ARCI), Balapur, Hyderabad, Telangana 500005, India

K. R. C. Soma Raju
e-mail: somarajuk@arci.res.in

R. Subasri
e-mail: subasri@arci.res.in

A. Gautam · K. V. Gobi
Department of Chemistry, National Institute of Technology Warangal, Warangal, Telangana 506004, India
e-mail: kvgobichem@nitw.ac.in

U. K. Mudali et al. (eds.), *Recent Trends in Electrochemical Science and Technology*, Springer Proceedings in Materials 15,
https://doi.org/10.1007/978-981-16-7554-6_1

methods, they are restricted for further use hereafter due to their toxicity and carcinogenic nature [4]. The most promising alternate method is the use of hybrid organic and inorganic silane-based sol–gel coatings [5]. Sol–gel coatings are highly stable, eco-friendly, and possess good adhesion and barrier properties, and they require only simple curing at relatively low temperatures [6]. Even though the sol–gel coatings form thick and homogeneous coatings on the metal substrates, these coatings get damaged and lose their barrier properties during long exposure times to aggressively corrosive media [7]. To overcome this drawback, imparting additional functionality to such simple, stable and easy-forming hybrid sol–gel coatings is highly preferred. Incorporation of corrosion inhibitors into sol–gel coatings is a recent strategy to produce self-healing coatings, which possess enhanced barrier properties for a longer duration in addition to anticorrosion properties [5]. In order to fabricate self-healing coatings, the self-healing agent can either be added directly into the matrix sol or nanocontainers entrapped (sealed) with corrosion inhibitors can be added into the sol–gel matrix. The direct addition of corrosion inhibitors can cause an excess of leaching, leading to unwanted reactions with the matrix. Hence, encapsulation is the better alternative. Nanocontainers encapsulated with corrosion inhibitors show controlled release and avoids excess leaching [8].

Different kinds of nanocontainers such as layered double hydroxides, layer-by-layer polyelectrolyte shells, nanoclays such as montmorillonite and halloysite, carbon nanotubes, polymeric nanocontainers, etc. have so far been investigated [9, 10]. Halloysite nanotubes (HNT) are widely used nanocontainers because they are easily available, eco-friendly, and cost-effective. Halloysite nanotubes are naturally occurring aluminosilicates, $Al_2Si_2O_5(OH)_4.2H_2O$, having a hollow lumen for easy entrapment of corrosion inhibitors. Halloysite nanoclay has a layered structure consisting of one alumina sheet and one silica sheet, as shown in Fig. 1a [11].

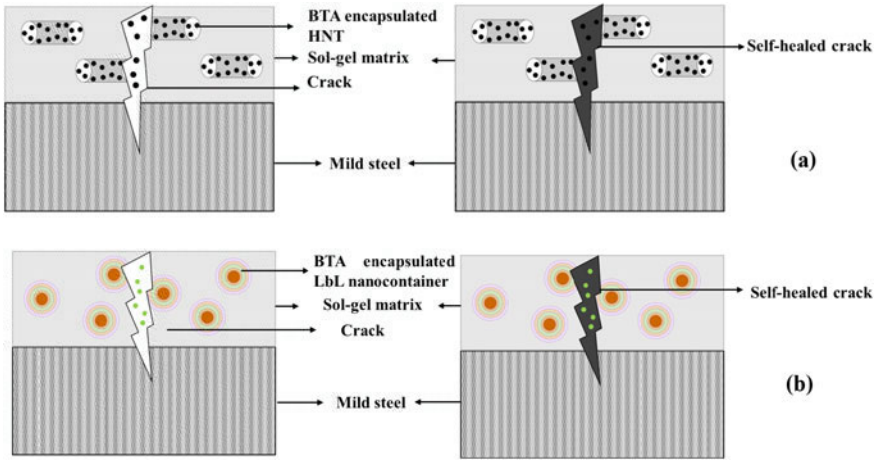

Fig. 1 Schematic of expected autonomic-healing process: **a** BTA encapsulated in HNT, **b** BTA encapsulated in LbL nanocontainers

Layer-by-layer (LbL) polyelectrolyte shell-based nanocontainers are also promising materials for entrapping the corrosion inhibitor within the polymeric shells. LbL approach involves the use of nanoparticles as a support system onto which polyelectrolyte layers of opposite charges are deposited. Corrosion inhibitors are entrapped in between the layers for their controlled release and thus provide more stability to the coating matrix, as depicted in Fig. 1b [12, 13].

The purpose of this research work is to examine the anticorrosion and self-healing behavior of eco-friendly hybrid sol–gel matrix dispersed with benzotriazole (BTA) encapsulated into two different types of nanocontainers, namely HNT and LbL polyelectrolyte shell. The encapsulation of BTA into different types of nanocontainers depends on the charge of the BTA molecule. Being an anionic inhibitor, it can bind easily with the hollow lumen of HNT which is positively charged because of the presence of the alumina layer inside. A similar effect is seen when BTA is loaded into LbL nanocontainers where BTA is entrapped in between the polyelectrolyte layers based on charge difference [14]. The effects of encapsulation of corrosion inhibitors dispersed into the sol–gel matrix on its barrier and mechanical properties are analyzed and discussed.

2 Experimental

2.1 Materials

For the synthesis of hybrid silane-based sol–gel matrix (3-Glyidyloxypropyl) trimethoxy silane (GPTMS, Alfa Aesar, Assay-97%) and tetraethyl orthosilicate (TEOS, purchased from Sigma Aldrich, USA, Assay-98%) precursors were used. Halloysite nanoclay (HNT, Sigma Aldrich, USA) was used as an encapsulating agent for corrosion inhibitors. Anionic polyacrylic acid (PAA) and cationic polydiallyl dimethyl ammonium chloride (PDADMAC) (Sigma Aldrich, USA) were used as the polyelectrolyte layered nanocontainers on Fe_2O_3 nanoparticles (supplied by Sigma Aldrich, USA) for encapsulating the self-healing material. Benzotriazole (SRL, Purity-97%) was used as self-healing material in both HNT and LbL nanocontainers. For coating deposition, mild steel coupons of dimensions 2.5 cm × 2.5 cm × 0.3 cm were used. The chemical composition of mild steel was found to be C: 0.18 wt%, Mn: 0.58 wt%, Si: 0.25 wt%, P: 0.018 wt%, S: 0.037 wt% and Fe: balance.

2.2 Preparation of Assembled Hematite-based LbL Nanocontainers

Standard polymer solutions of PAA and PDADMAC were prepared by dissolving polymer solution in deionized water of concentration 10 mg/mL. For layer-by-layer

assembly, PAA and PDADMAC were adsorbed on hematite particles at a concentration of 0.1 mg/mL. The first negatively charged layer of PAA was deposited on hematite particles by centrifuging at the speed of 6000 rpm for 15 min. The obtained powder was then re-dispersed and stirred in 0.1 M NaCl solution for 10 min and sonicated for 1 min in order to remove loosely bound particles. A similar procedure was followed for deposition of BTA (2 g/100 mL) which was followed by the deposition of the second layer of PAA. The fabrication of nanocontainers was terminated using a cationic polyelectrolyte layer of PDADMAC. The pH of all the solutions during the fabrication was maintained at 5.5 [14].

2.3 Loading of BTA in HNTs

For the synthesis of inhibitor-loaded HNT, 357 mg of BTA was added to 0.1 L of isopropyl alcohol (IPA) and subsequently, 5 g of HNT was added. The mixture was stirred for 20 min and evacuated at room temperature for 3 h. The obtained suspension was collected by centrifugation followed by oven drying at 50 °C for 20 min [15].

2.4 Sol Preparation and Coating Procedure

Matrix sol was synthesized by hydrolysis of GPTMS with TEOS in a mole ratio of 3.5:1 using hydrogen chloride (HCl) as catalyst followed by the addition of an optimized amount of self-healing agent. The sols were named as matrix (only for matrix sol), BLLS (loading the sol with BTA entrapped LbL nanocontainers), BS (loading the sol with BTA), BHS (loading the sol with BTA encapsulated HNT). For polishing the mild steel (MS) coupons 1000 grade sandpaper was used and was degreased using acetone in an ultrasonicator for 15 min. A dip-coater (EPG GmbH, Germany) was used to generate the coatings at a withdrawal speed of 0.1 cm/s and was cured at 130 °C for 60 min in a drying oven.

2.5 Characterization and Testing

Surface morphology and elemental composition of as-received hematite nanoparticles, HNT, and inhibitor-loaded nanocontainers were investigated using ZEISS Gemini 500 scanning electron microscope equipped with energy-dispersive X-ray spectroscopy (EDS) attachment. X-ray diffraction (XRD) was performed for as procured hematite nanoparticles using X-ray diffractometer (Bruker AXS D8 Advance, USA) in the 2θ range of 6°–100° with a step size of 0.1°. Zeta potential measurements for each deposited polyelectrolyte layer for LbL nanocontainers were

carried out using Zetasizer (MALVERN AT-0050007) instrument. Coating thickness was measured using gauge PosiTector® 6000 (De Felsko Corporation, USA). Multi-hatch gauge (BEVS 2203, China) according to ISO standard 2409 was used to perform the adhesion test and the substrates were then observed under an optical microscope (Olympus BX51M).

Electrochemical impedance and polarization studies for bare as well as coated mild steel coupons were carried out using the electrochemical analyzer from CH Instruments (Model CHI 604E, USA). The electrochemical cell consists of a three-electrode system with a saturated calomel electrode (reference electrode), platinum electrode (counter electrode), and the metal surface (working electrode). AC signal of 0.01 V amplitude was applied with frequency ranging from 100 kHz to 0.01 Hz to record the electrochemical impedance data. The bare and coated MS coupons were immersed in corrosive media of concentration 0.6 mol/L for 1 h before performing the polarization studies. A potential of ±300 mV was applied in accordance with open circuit potential at a scanning rate of 1 mV/s for conducting polarization measurements. The electrochemical impedance and polarization data were examined with the help of ZSimpWin and CH604E software. The salt spray test was performed by exposing the scribed coated and uncoated MS coupons to a highly corrosive environment for 24 h based on ASTM B117.

3 Results and Discussion

3.1 Scanning Electron Microscopy Analysis

SEM analysis for as-received α-Fe_2O_3 nanoparticles, corrosion inhibitor-loaded LbL nanocontainers, as procured halloysite nanotube and inhibitor-loaded halloysite nanotube was carried out. Elemental composition was determined using EDS. The FESEM image shown in Fig. 2 for as-received α-Fe_2O_3 nanoparticles reveals that the particles are in clusters having spherical structures with an average diameter of 30 nm. Fe and O were found as constituent elements from the EDS data as depicted in Fig. 2. The polyelectrolyte layer deposited α-Fe_2O_3 nanoparticles show large agglomerates of approximately 200 nm diameter, and EDS analysis indicates the presence of Fe, O, C, Na, Cl, and N confirming the formation of BTA entrapped polyelectrolyte layers on α-Fe_2O_3 nanoparticles. FESEM analysis of as-received HNT shows that the nanoclay has a tubular structure with transparent hollow lumen, and the elemental analysis reveals the presence of Al and Si elements in larger proportions. The inhibitor-loaded HNT shows denser and darker tubular structures, confirming the loading of BTA in the hollow lumen of HNT. Further, the elemental composition determined by EDS analysis shows the presence of Al, Si, C, and N, confirmed the entrapment of BTA in HNT.

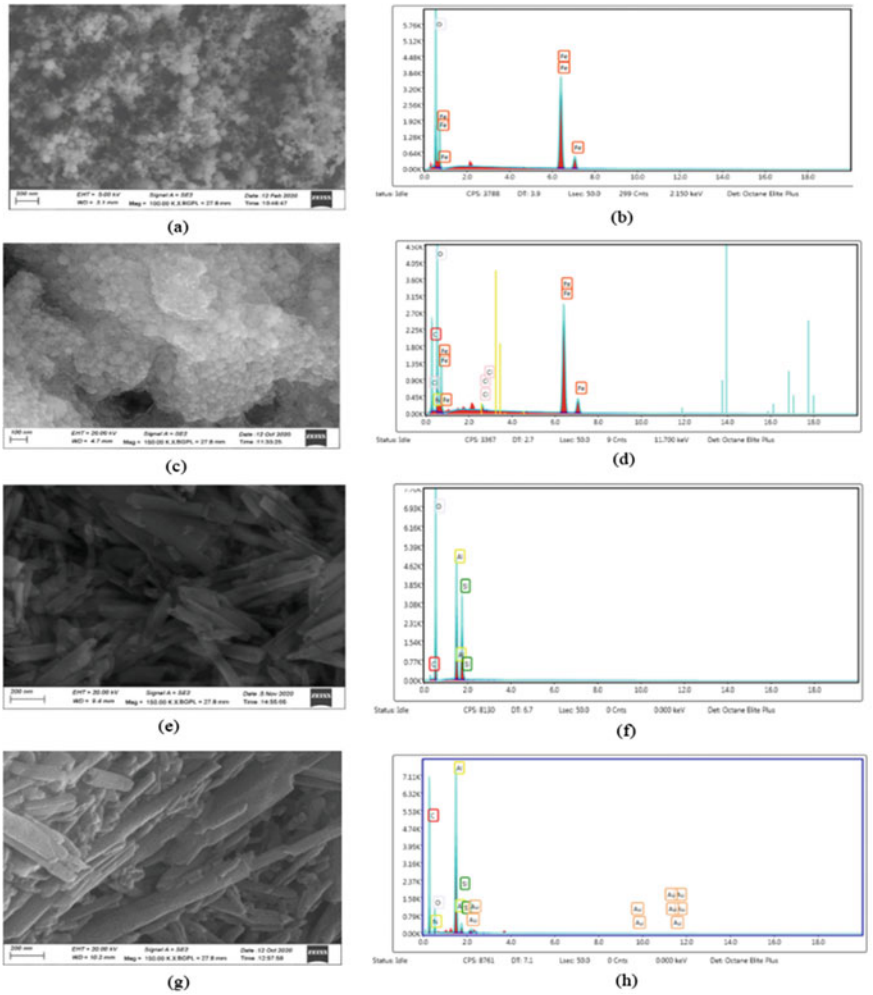

Fig. 2 FESEM images and EDS profiles: **a**, **b** Fe_2O_3 nanoparticles; **c**, **d** BTA entrapped polyelectrolyte layers deposited α-Fe_2O_3 nanoparticles; **e**, **f** HNT clay; **g**, **h** BTA encapsulated HNT nanoclay

3.2 X-Ray Diffraction

The XRD pattern for as-received α-Fe_2O_3 nanoparticles is shown in Fig. 3. The XRD analysis shows the intense peak at the 2θ value of 35°, indicating that the crystal structure of α-Fe_2O_3 is tetragonal, according to the International Centre for Diffraction Data (ICDD File no. 04-014-7214).

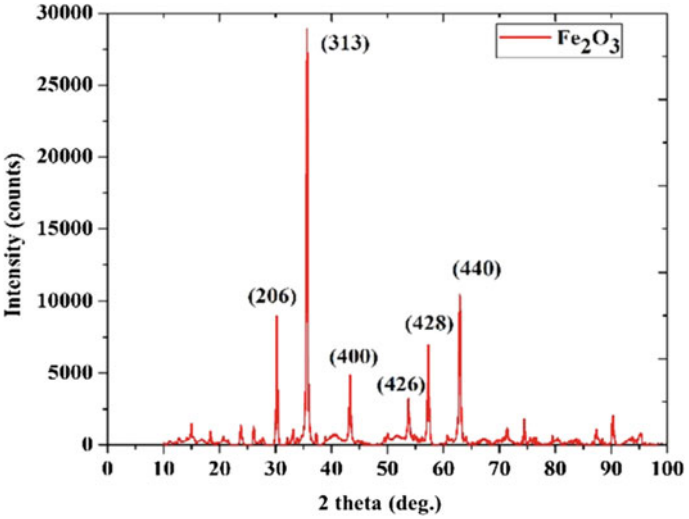

Fig. 3 XRD pattern for as-received Fe_2O_3 nanoparticles

3.3 Zeta Potential and Electrophoretic Mobility Measurements

Zeta potential and electrophoretic mobility were carried out for α-Fe_2O_3 nanoparticles along the several stages of stepwise depositions of polyelectrolyte layers using the Zetasizer instrument. Zeta potential values of α-Fe_2O_3 nanoparticles at all stages were found to be in the range of ±15 to ±30 mV, thereby confirming that the particles are highly stable without the formation of any agglomerates. The electrophoretic mobility confirmed that the α-Fe_2O_3 nanoparticles were found to be positively charged (Fig. 4). The negative electrophoretic mobility for PAA layer deposited nanoparticles confirmed that the negative surface charge surrounds the nanoparticles, confirming the firm deposition of the PAA layer on α-Fe_2O_3 nanoparticles. Entrapment of BTA on the PAA layer decreased the negative charge mobility values. The loosely bound particles of BTA were removed by depositing a second negatively charged layer of PAA. With the further deposition of a second PAA layer, the electrophoretic mobility value became a little more negative. The nanocontainers were terminated using the cationic polyelectrolyte layer of PDADMAC, and hence the electrophoretic mobility for this layer was found to be positive, as depicted in Fig. 4. The zeta potential measurements confirmed that the surface charge of each deposited layer was in accordance with the charge of each layer and the particles are stable in nature. The observed results of zeta potential and electrophoretic mobility studies supported the stepwise deposition of polyelectrolyte layers and the fabrication of LbL nanocontainers, and the results are in good agreement with the literature report [14].

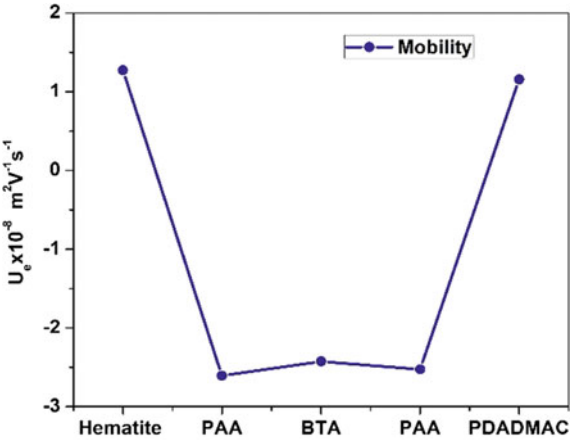

Fig. 4 Comparison of electrophoretic mobilities of each deposited layer

3.4 Thickness and Adhesion Measurements

The thicknesses of matrix, BS, BLLS, and BHS sol–gel coatings were found to be in the range of 6–8 microns. Adhesion test was carried out using a multi-hatch gauge where crosshatches were marked manually. The images obtained using an optical microscope before and after the adhesion test are shown in Fig. 5. For all the coatings, the adhesion test showed that no coating was removed from the corners of each intersection point of the crosshatch. The corners and edges of the squares were smooth. Hence, the observations confirm that all the coatings possess good adhesion properties with the substrate in accordance with the ISO standard 2409, where such types of coatings are classified into 0 class (means 0% removal).

3.5 Electrochemical Impedance Spectroscopy (EIS) and Potentiodynamic Polarization Studies (PPS)

EIS along with PPS was conducted for bare and coated MS substrates exposed to 0.6 mol/L NaCl solution for 1 h. The data obtained after the electrochemical measurements were studied using two different equivalent electric circuits, shown in Fig. 6. The equivalent circuit impedance parameters are R_s (resistance due to solution), CPE_{coat} (capacitance due to coating) R_{coat}, (resistance due to coating), C_{edl} (capacitance due to electrical double layer), and R_{ct} (resistance due to charge transfer). Figure 6a conveys the equivalent electric circuit that fitted best for bare substrate, where R_s is connected in series with CPE_{edl} and R_{ct} which are in parallel with each other. In order to obtain the EIS parameters for coated substrates with and without encapsulating BTA into the nanocontainers, the equivalent electric circuit shown in Fig. 6b fitted best. Here, the R_s is in series with CPE_{coat} parallel to R_{coat},

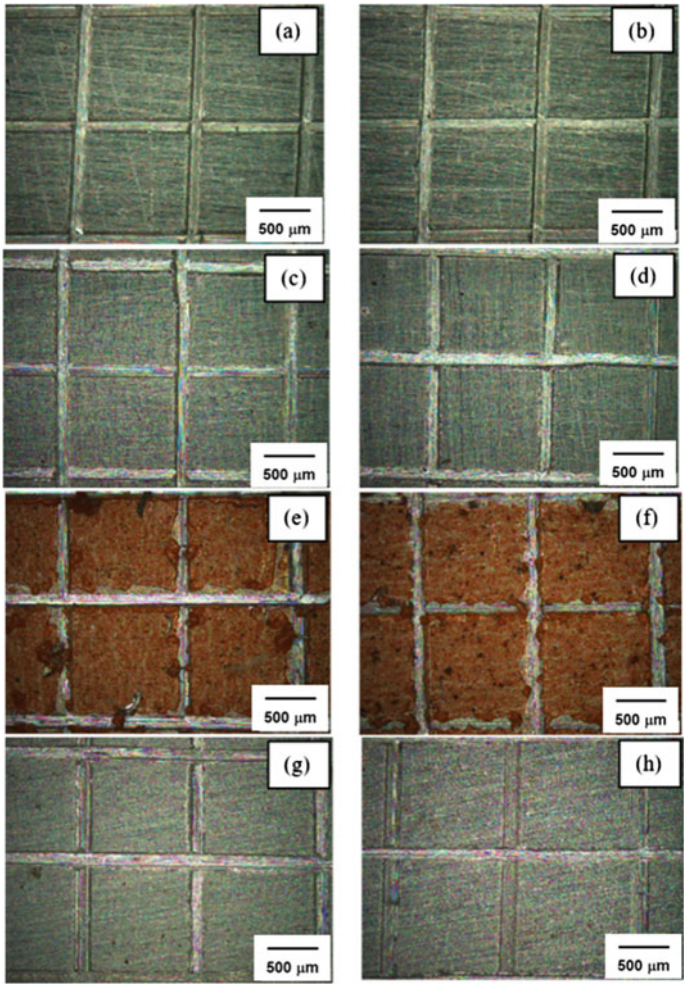

Fig. 5 Tape adhesion test images of different coatings **a**, **b** matrix sol, **c**, **d** BS, **e**, **f** BLLS, and **g**, **h** BHS coupons

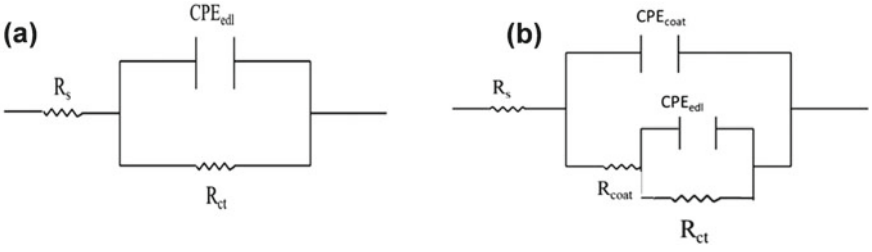

Fig. 6 Equivalent electric circuits for **a** bare and **b** coated coupons

which are in series with C_{edl} parallel to R_{ct}. Since the Nyquist plot obtained deviates from the standard semicircle shape, the CPE (constant phase element) was used instead of a pure capacitor for all the circuit fittings. Presence of intrinsic surface non-uniformity of mild steel is responsible for the non-ideal nature of the electrical double layer. The pseudocapacitance value can be obtained using the formula:

$$C = (Q_o * R)^{1/n}\left(1/R\right)$$

where C is pseudocapacitance in F/cm^2, Q_o is constant phase element in S-sec^n/cm^2, n is frequency factor and R is resistance in Ω.

The Nyquist plots obtained after 1 h exposure to NaCl solution of concentration 0.6 mol/L are displayed in Fig. 7. The plots obtained for bare and coated coupons are nearly semicircular in shape, showing good corrosion resistant properties. The impedance value for bare substrate was found to be very low, from which it can be inferred that it has very low corrosion resistance. Hybrid sol–gel coating and added corrosion inhibitor can be responsible for increased impedance values of matrix and BTA loaded matrix coated substrates, attributing to the larger diameter of the semicircle. The sol–gel coating consisting of BTA encapsulated LbL nanocontainers (BLLS) showed higher impedance values and larger semicircle compared to the only matrix coated and BS coated substrates, thereby exhibiting higher corrosion resistance and lower corrosion rate. The BTA-HNT-sol coated substrates (BHS) exhibited enhanced corrosion resistance with impedance values several orders higher than those of all other coatings, indicating the extremely superior corrosion resistance and barrier properties of BHS coatings. The electrochemical impedance data along with

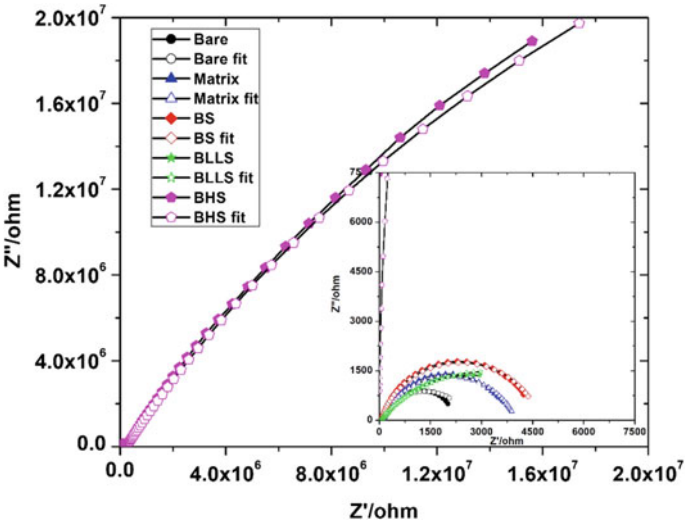

Fig. 7 Nyquist plots for bare and coated coupons

charge transfer resistance values are shown in Table 1. The data obtained show that the capacitance value for BLLS coated substrates has increased when compared to the only matrix coated substrates which can be because of the presence of polyelectrolyte layers that swell upon absorption of water and acts as a barrier by blocking the entry of foreign species. With time, these polyelectrolyte layers may burst with an increase in water uptake initiating the release of encapsulated corrosion inhibitor which self-heals the damage on the metal surface thereby confirmed from the coating resistance value. The BS coated substrates have shown an increase in coating capacitance because of the uptake of water along with an increase in coating resistance which can be attributed because of the presence of freely loaded BTA into the matrix sol which adsorbs on the mild steel surface at the sites where Cl^- ions of the electrolyte solution was attached. This results in the formation of a protective film that restricts the entry of water molecules to some extent. The BHS coated substrates have shown a decrease in capacitance value suggesting that the coating is more compact which blocks further penetration of water molecules. This barrier film formation protects the metal surface from corrosion. The coating and charge transfer resistance values have increased drastically for BHS coated substrates when compared to other coatings. The corrosion inhibitor molecules get protonated in presence of electrolyte solution which forms a bond with the negatively charged surface of the metal. This interaction helps in corrosion mitigation by self-healing the defects on the metal surface [16].

Potentiodynamic polarization profiles of bare and coated substrates after 1 h exposure to 0.6 mol/L NaCl solution were recorded and are shown in Fig. 8. The values of corrosion potential and corrosion current are shown in Table 2. The data reveal that the corrosion potential values changed a meager by 60 mV from bare electrodes and became more positive for sol-gel coatings (Matrix and BS) and more negative for nanocontainer encapsulated substrates (BLLS and BHS). However, the value of corrosion current was high for bare, matrix, and BS substrates, but the nanocontainer encapsulated coatings (BLLS and BHS) exhibited low corrosion currents. This extreme decrease in corrosion current established the enhanced self-healing ability provided by BTA entrapped HNT sol coating. The encapsulated BTA-HNT sol (BHS) coated substrates exhibited extremely low corrosion current density and hence very low corrosion rate, indicating that the controlled release of BTA from HNT provided better self-healing properties and good corrosion resistance when compared to uncoated and other coated substrates.

Table 1 EIS fit data for bare and coated substrates after 1 h exposure to 0.6 mol/l NaCl solution

Substrate	R_{coat} ($\Omega.cm^2$)	R_{ct} ($\Omega.cm^2$)	C_{coat} (F/cm^2)	C_{edl} (F/cm^2)	χ^2
Bare	–	2558	–	4.280×10^{-4}	5.369×10^{-3}
Matrix	158.1	3813	1.599×10^{-5}	5.614×10^{-5}	3.579×10^{-3}
BS	726.8	3955	1.012×10^{-4}	1.11×10^{-5}	3.076×10^{-3}
BLLS	438.4	5954	7.343×10^{-5}	1.189×10^{-5}	4.801×10^{-3}
BHS	2.287×10^5	$1.03\ 3 \times 10^8$	2.178×10^{-10}	7.478×10^{-7}	6.490×10^{-3}

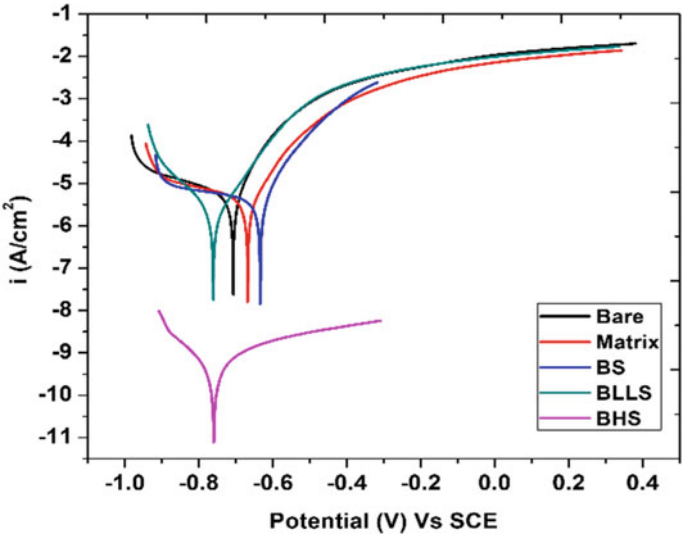

Fig. 8 Tafel plots for bare and coated coupons

Table 2 Electrochemical polarization data for bare and coated coupons

Substrate	E_{corr} (V vs. SCE)	I_{corr} (A/cm^2)
Bare	−0.707	5.54×10^{-6}
Matrix	−0.668	5.37×10^{-6}
BS	−0.634	4.86×10^{-6}
BLLS	−0.761	2.25×10^{-6}
BHS	−0.760	5.35×10^{-10}

3.6 Salt Spray Test

Photographs of uncoated and coated substrates after salt spray test are shown in Fig. 9. Artificial scribes were created on the coated substrates in order to visualize the self-repairing nature of the coatings. The substrates were kept in a salt spray compartment and exposed to 5 wt% NaCl solution for different time durations namely, 1, 2, 4, 6 and 24 h. The images obtained after 1 h exposure show that the corrosion products are formed on the bare substrate, whereas, for the coated substrates, no significant change was observed. After 2 h exposure, the bare substrate was 50% corroded but the matrix coated substrate showed the rust formation at the edges of the defect and nearby area. The BTA loaded coatings still possessed good corrosion inhibition properties. Images obtained after 4 and 6 h exposure clearly showed that the bare substrate got corroded completely, whereas matrix, BS, and BHS coated substrates were nearly 50% corroded, which indicates that the barrier feature of the matrix-coated substrates prevents the penetration of foreign electrolyte species enabling the protection of

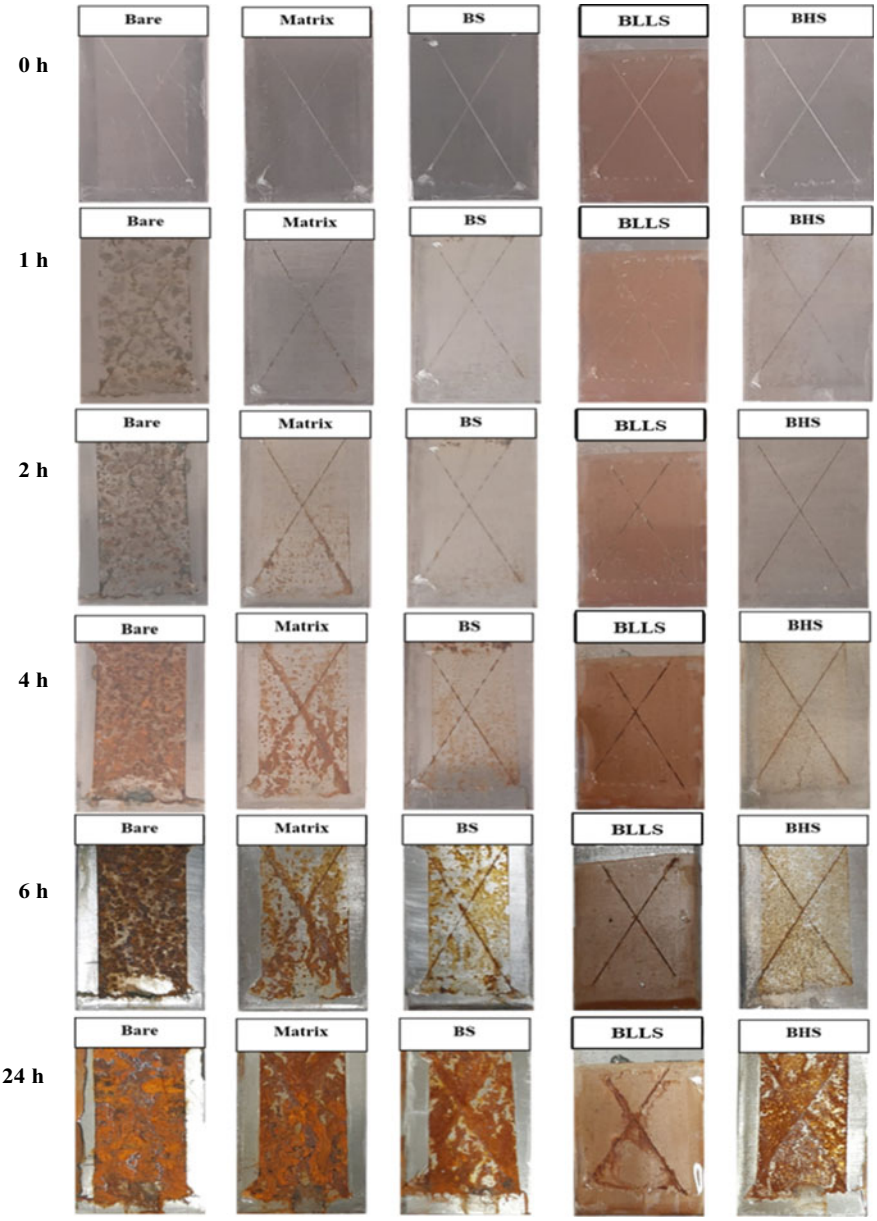

Fig. 9 Images of bare and coated MS substrates when exposed to salt spray

MS substrates to some extent whereas, loading of BTA into the sol delivered self-healing behavior as the inhibitor is released from the scribed area. Images obtained after 24 h exposure illustrate that all the substrates got corroded completely but the BLLS-sol coated substrate showed enhanced barrier properties because of the layered structure, where the polyelectrolyte layers swell up on absorbing the electrolyte solution imparting protection for longer durations when compared to other coatings. In addition, BTA acts as the next step for protection by self-healing the surface defects.

The information obtained from SST differs from EIS and PPS. The reason behind this difference is that the SST is an accelerated test where artificial defects are made on the coatings to observe the self-healing mechanism of bare and coated substrates, whereas, in EIS technique, no such damage occurs and information is retrieved based on the adhesion of coatings onto the metal surface. The PPS measures the stability of the system when polarized with respect to open circuit potential. Therefore, the BLLS coated substrates have shown enhanced barrier properties when compared to other coatings because of the presence of a layered structure where the polyelectrolyte layers swell upon uptake of water. These polyelectrolyte layers on increase in pressure may burst which in turn releases the corrosion inhibitor imparting the self-healing behavior for longer durations. Similar effect was observed where the capacitance values have increased because of the water uptake.

4 Conclusions

- Hybrid sol–gel coatings exhibited good barrier properties by forming homogenous coatings on substrates.
- BTA encapsulated halloysite nanotubes when mixed in sol–gel matrix showed enhanced corrosion protection properties when exposed to 0.6 mol/L NaCl solution.
- Electrochemical impedance and polarization studies revealed higher corrosion resistance and lower corrosion rate for coatings containing BTA encapsulated in halloysite nanoclay among all coated substrates.
- The salt spray analysis confirmed the self-healing behavior of encapsulated BTA into HNT for up to 6 h. The BLLS-sol coated substrates showed good barrier properties up to 24 h when subjected to SST (salt spray test) because of the presence of polyelectrolyte layers which swell up and restricts the entry of water molecules. In addition to this, the encapsulated BTA provides protection by self-healing the damage.

Acknowledgements The authors are thankful to Director, ARCI for all support throughout the investigation carried out. The authors would like to acknowledge Dr. K. Suresh and Balaji Padya for XRD and Zeta potential measurements.

References

1. Basik M, Mobin M (2020) Chondroitin sulfate as potent green corrosion inhibitor for mild steel in 1 M HCl. J Mol Struct 1214:128231. https://doi.org/10.1016/j.molstruc.2020.128231
2. Hamidon TS, Hussin MH (2020) Susceptibility of hybrid sol-gel (TEOS-APTES) doped with caffeine as potent corrosion protective coatings for mild steel in 3.5 wt.% NaCl. Prog Org Coat 140:105478. https://doi.org/10.1016/j.porgcoat.2019.105478
3. Zhao J, Xia L, Sehgal A, Lu D, McCreery RL, Frankel GS (2001) Effects of chromate and chromate conversion coatings on corrosion of aluminum alloy 2024–T3. Surf Coat Technol 140:51–57. https://doi.org/10.1016/S0257-8972(01)01003-9
4. Zheludkevich ML, Tedim J, Ferreira MGS (2012) "Smart" coatings for active corrosion protection based on multi-functional micro and nanocontainers. Electrochim Acta 82:314–323. https://doi.org/10.1016/j.electacta.2012.04.095
5. Figueira RB, Fontinha R, Silva CJR, Pereira EV (2016) Hybrid sol-gel coatings: smart and green materials for corrosion mitigation. Coatings 6:12. https://doi.org/10.3390/coatings6010012
6. Figueira RB, Silva CJR, Pereira EV (2014) Organic–inorganic hybrid sol–gel coatings for metal corrosion protection: a review of recent progress. J Coat Technol Res 12:1–35. https://doi.org/10.1007/s11998-014-9595-6
7. Li Y, Wu C, Xue M, Cai J, Huang Y, Yang H (2019) Preparation of sol-gel derived anticorrosive coating on Q235 carbon steel substrate with long-term corrosion prevention durability. Materials (Basel) 12:1960. https://doi.org/10.3390/ma12121960
8. Habib S, Khan A, Nawaz M, Sliem MH, Shakoor RA, Kahraman R, Abdullah AM, Zekri A (2019) Self-healing performance of multifunctional polymeric smart coatings. Polymers (Basel) 11:1519. https://doi.org/10.3390/polym11091519
9. Nazeer AA, Madkour M (2018) Potential use of smart coatings for corrosion protection of metals and alloys: A review. J Mol Liq 253:11–22. https://doi.org/10.1016/j.molliq.2018.01.027
10. Ghazi A, Ghasemi E, Mahdavian M, Ramezanzadeh B, Rostami M (2015) The application of benzimidazole and zinc cations intercalated sodium montmorillonite as smart ion exchange inhibiting pigments in the epoxy ester coating. Corros Sci 94:207–217. https://doi.org/10.1016/j.corsci.2015.02.007
11. Izadi M, Mohammadi I, Shahrabi T, Ramezanzadeh B, Fateh A (2019) Corrosion inhibition performance of novel eco-friendly nanoreservoirs as bi-component active system on mild steel in aqueous chloride solution. J Taiwan Inst Chem Eng 95:555–568. https://doi.org/10.1016/j.jtice.2018.09.012
12. Rydzek G, Ji Q, Li M, Schaaf P, Hill JP, Boulmedais F, Ariga K (2015) Electrochemical nanoarchitectonics and layer-by-layer assembly: From basics to future. Nano Today 10:138–167. https://doi.org/10.1016/j.nantod.2015.02.008
13. Sonawane SH, Bhanvase BA, Jamali AA, Dubey SK, Kale SS, Pinjari DV, Kulkarni RD, Gogate PR, Pandit AB (2012) Improved active anticorrosion coatings using layer-by-layer assembled ZnO nanocontainers with benzotriazole. Chem Eng J 189–190:464–472. https://doi.org/10.1016/j.cej.2012.02.076
14. Kamburova K, Boshkova N, Boshkov N, Radeva T (2016) Design of polymeric core-shell nanocontainers impregnated with benzotriazole for active corrosion protection of galvanized steel. Colloids Surf A Physicochem Eng Asp 499:24–30. https://doi.org/10.1016/j.colsurfa.2016.03.067
15. Abdullayev E, Lvov Y (2011) Halloysite clay nanotubes for controlled release of protective agents. J Nanosci Nanotechnol 11:10007–10026. https://doi.org/10.1166/jnn.2011.5724
16. Njoku DI, Cui M, Xiao H, Shang B, Li Y (2017) Understanding the anticorrosive protective mechanisms of modified epoxy coatings with improved barrier, active and self-healing functionalities: EIS and spectroscopic techniques. Sci Rep 7:1–15. https://doi.org/10.1038/s41598-017-15845-0